Yu, S., & Zhang, Y. (2017). High efficiency wide band SiNx-on-SOI grating coupler with low fabrication complexity. *Optics Letters*. https://doi.org/10.1364/OL.42.003391

High efficiency wide band SiN_x-on-SOI grating coupler with low fabrication complexity

PENGFEI XU[1], YANFENG ZHANG[1,*], ZENGKAI SHAO[1], LIN LIU[1], LIDAN ZHOU[1], CHUNCHUAN YANG[1], YUJIE CHEN[1], AND SIYUAN YU[2,*]

[1]*State Key Laboratory of Optoelectronic Materials and Technologies, School of Electronics and Information Technology, Sun Yat-sen University, Guangzhou 510275, China*
[2]*Photonics Group, Merchant Venturers School of Engineering, University of Bristol, Bristol BS8 1UB, UK*
**Corresponding author: zhangyf33@mail.sysu.edu.cn*

Received XX Month XXXX; revised XX Month, XXXX; accepted XX Month XXXX; posted XX Month XXXX (Doc. ID XXXXX); published XX Month XXXX

Chip-fiber grating coupler is a fundamental building block in integrated photonics, providing convenient on-wafer testing and packaging. Couplers based on silicon nitride (SiN_x) material platform can achieve wider bandwidth than silicon-based couplers, but suffers from lower efficiency due to the relative low material refractive index. The efficiency of SiN_x grating coupler can be improved by using high reflectivity silicon grating reflectors underneath. However, such silicon grating reflector requires several fabrication steps, including lithography, etching, high precision alignment (HPA), and chemical mechanical polishing (CMP). In this work, we demonstrate an easy-to-fabricate SiN_x-on-SOI TE mode grating coupler requiring only one patterning step (grating alone), and without the need of HPA and CMP. A coupling coefficient of -2.5 dB and 1-dB-bandwidth of 65 nm have been experimentally measured.

OCIS codes: *(250.5300) Photonic integrated circuits; (350.2770) Gratings;*

http://dx.doi.org/10.1364/OL.99.099999

Silicon photonic waveguides [1], while benefit from high material refractive index, are very sensitive to fabrication quality and is also susceptible to a number of material limitations. Silicon nitride (SiN_x) proved to be a promising supplement to silicon photonics due to its low propagation loss, negligible two-photon absorption, wide transparency window extended to visible spectral range, moderate refractive index, and CMOS-compatible fabrication process [2,3]. SiN_x thin films not only can be deposited using conventional low-pressure chemical vapor deposition (LPCVD), it can also be deposited using plasma-enhanced chemical vapor deposition (PECVD) in low temperature condition, which makes it more widely compatible with various substrates and processes [4-6]. SiN_x is therefore a promising candidate in many applications, including microwave photonics [7-10], mid-infrared [11-13], nonlinear optics [14,15], quantum optics [16], bio-sensing [17], and super-resolution optical microscopy [18]. In addition, SiN_x can also be used in the hetero-integration platform to support furthermore functionalities, for example, photo-detection [19] and quantum interference [20].

The moderate refractive index (n~2) of the SiN_x, while effectively increasing the fabrication tolerance, improving the conformity and reducing the channel cross-talk in a complex photonic system [21], can become a limiting factor for the coupling efficiency of vertical grating couplers, where high index contrast is key to the effective scattering of light within the region matching to the single mode fiber.

Table1. Recently published SiN_x grating couplers aimed at the use in the wavelength region of C band.

Coupler design	1-dB BW (nm)	Peak eff. (dB)	Etch step	CMP	HPA	Ref.
Conventional	50	-5.8	1	×	×	[5]
Conventional	60	-5.1	1	×	×	[22]
Conventional	67	-4.2	1	×	×	[23]
Inverse taper	54	-3.7	2	×	√	[24]
Bottom DBRs	53	-2.5	1	×	×	[25]
Bottom grating	80	-1.3	3	√	√	[26]
Bottom grating	40	-0.88*	2	√	√	[27]
Staircase grating	40	-0.66*	2	×	√	[28]
Bottom grating	65	-2.5	1	×	×	This work

The * marks represent simulation results.

Table 1 summarizes the 1-dB-bandwidth and peak efficiency of recently reported high efficiency SiN_x grating coupler design schemes for the use in C band in literature. Conditions representing fabrication complexity of those gratings, including the number of etching steps (grating alone), requirement of using CMP and/or HPA, are listed for comparison. For conventional grating couplers (i.e. single layer SiN_x grating), the fabrication process is simple but the peak coupling efficiency in experiment is limited to be -4~-6 dB. Note that using special designs may increase the coupling efficiency up to be better than -1 dB [27,28].

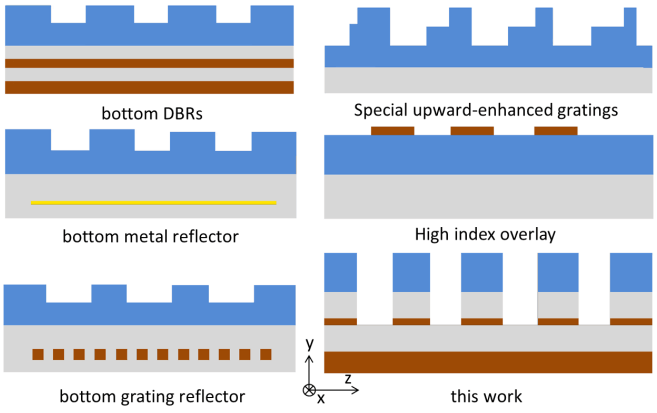

Figure 1. Various design strategies of high efficiency SiN_x or silicon grating couplers.

Most design schemes are mainly using the following strategies: bottom reflectors, special upward-enhanced gratings, and high index overlay, which are shown in Fig. 1. These schemes are employed primarily to increase the upward directionality of the optical power. However, these efficient schemes often require complex fabrication flows. For example, the bottom silicon grating reflector scheme is notable for extremely high efficiency (theoretically can be better than -1 dB) [27,28]. However, it requires multiple lithography, etching, HPA and CMP steps which are time-consuming and low tolerance.

To improve fabrication practicality whilst maintaining high coupling efficiency, we proposed a SiN_x-on-SOI grating coupler that requires only a single etching step, of which diagram is shown in Fig. 2. The proposed grating coupler is based on a commercially available standard SOI wafer with a 220-nm silicon thin layer and a 2-μm buried oxide (BOX) layer. An upper silicon oxide (SiO_2) buffer and a SiN_x waveguide layer are deposited on the SOI wafer by PECVD. The SiN_x-on-SOI grating is patterned by e-beam lithography (EBL) and etched in a single step through the SiN_x waveguide, the upper SiO_2 buffer, and the silicon thin layer.

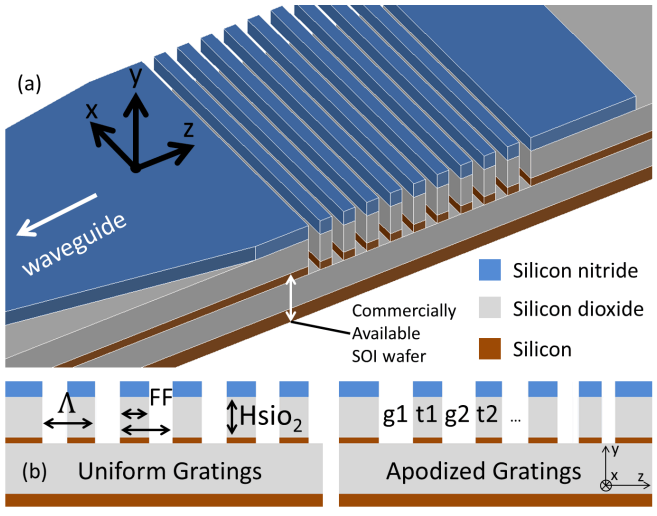

Figure 2. (a) Proposed SiN_x-on-SOI grating coupler. (b) The uniform and apodized grating coupler with the corresponding parameters illustrated in the diagram.

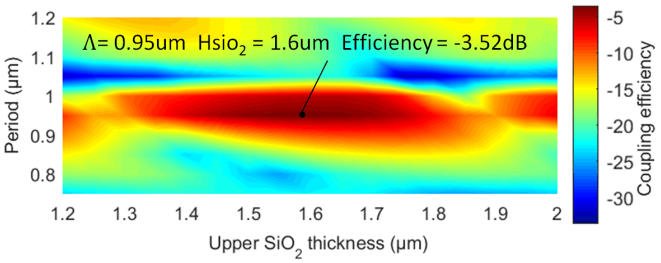

Figure 3. The coupling efficiency of the uniform grating with different grating period Λ and SiO_2 interlayer thickness *H*sio2.

The first design step is the optimization of a uniform grating. The following parameters are used: SiN_x thickness of 600 nm, gratings fill factor (FF) of 0.5, and refractive indices of silicon, SiO_2, SiN_x are 3.42, 1.9896, and 1.4431, respectively. The efficiency versus grating period Λ and the SiO_2 buffer thickness $H\text{sio}_2$ is mapped in Fig. 3. The maximum efficiency of – 3.52 dB can be obtained when the SiO_2 buffer thickness is 1.6 μm and the grating period is 0.95 μm.

The coupling efficiency of the uniform grating coupler is limited due to the mode mismatch between upward radiation and the transverse mode of the single mode fiber (SMF). Apodization is employed to further increase the coupling efficiency of the grating coupler. In the apodization process, the grating spacing is set to be >400 nm in order to ensure the plasma etching uniformity.

A genetic algorithm is performed to optimize both the mode-matched efficiency and the 1-dB bandwidth simultaneously enabling that the maximum efficiency-bandwidth product is achieved. The rigorous efficiency-bandwidth optimization is supposed to consider coupling efficiencies in a wide range of wavelength region to predict the efficiency-bandwidth, which, however, is time-consuming. Therefore, in order to reduce the calculation time, the efficiency of multiple wavelength with discrete spacing of 10 nm within the C band are considered, and the approximate efficiency-bandwidth product can be estimated and then optimized. The genetic algorithm optimization starts with a uniform grating, and continuously tunes all the parameters listed in table 2 with a step size of 5 nm, while the total upward optical power is recorded and the mode overlap integral is performed as [28]

$$\eta = \frac{\left|\int E_{up}^{*} E_{\mathrm{SMF}} dz\right|^2}{\int \left|E_{\mathrm{up}}\right|^2 dz \int |E_{SMF}|^2 dz} \qquad (1)$$

where E_{up} represents the distribution of the upward electric field, and E_{SMF} is the fundamental mode in the SMF, which can be approximately given as the tilt Gaussian form [30]:

$$E_{\mathrm{FIB}} = A \exp\left(-\frac{(z-z_0)^2}{w_0^2}\right) \exp\left(-jn\frac{2\pi}{\lambda}\sin\theta\, z\right) \qquad (2)$$

where the constant A represents the normalized amplitude of the Gaussian beam. The beam waist $w_0 = 5.2$ μm in this work. In the tilt term of the second exponential part of Eq. (2), the refractive index of the fiber core is set as $n = 1.46$ with a tilt angle $\theta = -8°$.

The coupling efficiency can be calculated by the upward power multiplied by the mode overlap coefficient. When the efficiency-bandwidth product is improved, the tuning parameter will be recorded as positive and preserved, otherwise the tuning

parameter will be considered as negative and discarded. The optimized grating parameters are listed in table 2.

Table 2. Parameters of the apodized grating coupler optimized by genetic algorithm (units: nm).

g1	t1	g2	t2	g3	t3	g4	t4
405	530	450	490	470	505	460	520
g5	t5	g6	t6	g7	t7	g8	t8
545	440	555	475	495	475	515	460
g9	t9	g10	t10	g11	t11	g12	$Hsio_2$
525	540	465	415	510	495	430	1625

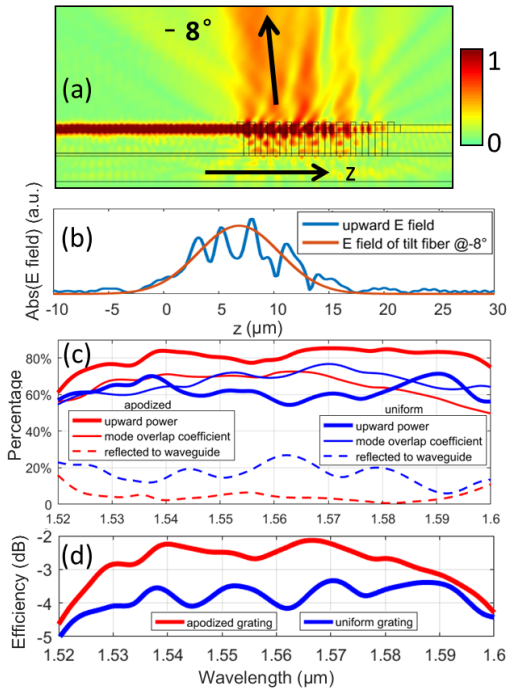

Figure 4. (a) Electric Field of the grating coupler numerically simulated by 2D-FDTD method. (b) Upward electric field matched with the tilted fiber mode profile. (c) Characteristics of the apodized and uniform grating coupler, and the upward diffraction power of apodized gratings can be increased to about 85% . (d) Simulated coupling efficiency of the grating couplers.

Figure 4(a) shows the simulated electric field distribution of the apodized grating coupler. With a coupling transverse electric (TE) fundamental mode from the left side of the SiN_x waveguide, the majority of the electric field is diffracted upward and matches the SMF mode. A slightly-tilted (-8 degree) vertical coupling is employed. It is noticed that in our simulation results, the negative coupling angle can have a better coupling performance than a positive one. Figure 4(b) demonstrates a good match between the upward field and the tilted SMF mode, and employing the genetic algorithm, the mode overlap coefficient can be increased up to ~73%. The upward power percentage can be as high as 85% [Fig. 4(c)]. Then the coupling coefficient in Fig. 4(d) is calculated using Eq. (1), indicating a simulated peak coupling efficiency of -2.13 dB at the center wavelength of 1567 nm, and an estimated 1-dB-bandwidth of about 63 nm. Due to the deep-etched grating configuration, when trying to increase the upward scattering power, the reflectance of the uniform grating is subsequently increased. However, in an apodized grating couplers, the upward power is maximized, and then the reflectance can be suppressed to a level lower than 5%.

In Fig. 5, the fabrication flow of the grating is presented. In order to achieve the deep etch of the stacked layers, a 250-nm-thick Chromium (Cr) metal mask is employed to achieve a simple and repeatable grating etching process, sufficiently thick to withstand the etching processes through three layers (SiN_x, SiO_2, and Si).

In the first etching stage, the SiN_x layer is etched by trifluoromethane (CHF_3) and oxygen plasma in a Reacted Ion Etching (RIE) chamber, followed by the second stage using CHF_3 and Argon (Ar) plasma to etch down the 1.6-μm-thick SiO_2 layer. In the 2nd stage, the RIE RF power must be reduced to about half of the ordinary level, in order to dilute the plasma concentration in the chamber, so that the physical and chemical etching can be re-balanced in the deep grating grooves. The final etching stage of the silicon layer is finished in an Inductive Coupling Plasma (ICP) chamber, using high density Hydrogen Bromide (HBr) plasma with fast silicon etching speed. The whole etching process can be completed within one hour.

The optical image of the fabricated sample taken under microscope is shown in Fig. 6(a). The SEM image of the etched profile is shown in Fig. 6(b). In our experiment, we apply the test scheme as that using a waveguide with grating coupler at one end and a cleaved facet at the other end. The fiber-to-fiber transmissivity is measured using a Keysight 8164B lightwave measurement system. The Bézier curve waveguide bends are employed to avoid the mode perturbation during the propagation which can improve the testing accuracy and reliability [31].

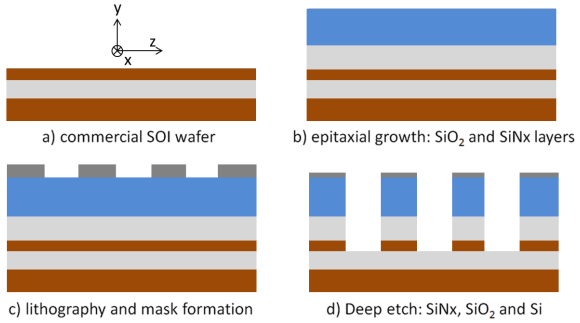

Figure 5. Fabrication flow of the gratings: (a) SOI wafer, (b) Deposited 1600 nm upper SiO_2 buffer layer and 600 nm SiN_x layer, (c) E-beam lithography and Cr lift-off to form the hard-mask, (d) Plasma etching, followed by Cr mask removal.

The extra insertion loss of about 4 dB, which is due to the combined losses of propagation loss in both SiN_x waveguide and SMFs, as well as losses caused by polarization controller and end coupling, has been calibrated and removed in the post data processing. The curves for revealing the relationship between the coupling efficiency and the wavelength for simulated and the fabricated grating couplers are plotted in Fig. 7. A peak coupling coefficient of -2.5 dB and a 1-dB-bandwidth of 65 nm can be achieved in the apodized grating, while the uniformed grating with Λ = 965 nm and FF = 51.3% can provide a peak coupling coefficient of -3.6 dB and a 1-dB-bandwidth of 70 nm, with the measurement results closely agreeing with the simulation.

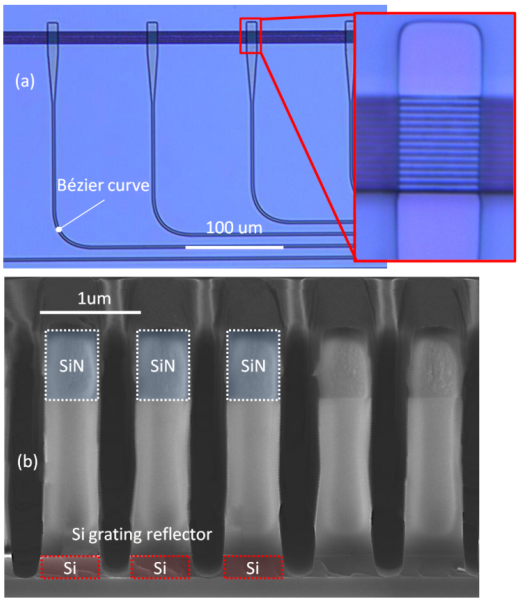

Figure 6. (a) SiN_x waveguides with the grating couplers for experimental measurement. (b) SEM cross-section of the fabricated SiN_x-on-SOI grating coupler.

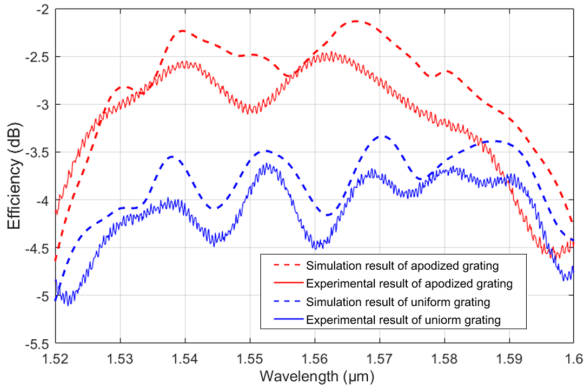

Figure 7. Experimental test of the grating coupler is performed and -2.5 dB coupling loss with 65 nm 1-dB-bandwidth can be achieved in the apodized grating, and -3.6 dB coupling loss with 70 nm 1-dB-bandwitdh can be obtained in the uniform grating.

In conclusion, we have proposed and experimentally demonstrated a new design scheme of high efficiency grating couplers for SiN_x waveguides that is simple to fabricate. A numerically optimized uniform grating design is first designed, and further optimized by means of a genetic-algorithm to achieve an apodized design. The fabrication process requires only one lithography step, and all layers are pre-deposited and etched in one self-aligned process. No surface polishing and accurate overlaying are needed, making it competitive in future practical production. The close matching between the simulation and measurement results also confirms the robustness of the design.

Funding. National Key Research and Development Program of China (No. 2016YFB0402503); National Basic Research Program of China (973 Program) (2014CB340000); National Natural Science Foundations of China (Nos. 61323001, 11690031, 61490715, 51403244); Natural Science Foundation of Guangdong Province (2014A030313104); Science and Technology Program of Guangzhou (201707020017); Fundamental Research Funds for the Central Universities of China (Sun Yat-sen University: 17lgzd06, 16lgjc16, 15lgpy04, 15lgzs095, 15lgjc25).

References

1. D. Thomson, A. Zilkie, J. E. Bowers, T. Komljenovic, G. T. Reed, L. Vivien, D. Marrismorini, E. Cassan, L. Virot, and J. M. Fédéli, J. Opt. **18**, 073003 (2016).
2. S. Romerogarcía, F. Merget, F. Zhong, H. Finkelstein, and J. Witzens, Opt. Lett. **38**, 2521-2523 (2013).
3. A. Rahim, E. Ryckeboer, A. Subramanian, S. Clemmen, B. Kuyken, A. Dhakal, A. Raza, A. Hermans, M. Muneeb, and S. Dhoore, J. Lightwave Technol. **35**(4), 639-649 (2017).
4. Z. Shao, Y. Chen, H. Chen, Y. Zhang, F. Zhang, J. Jian, Z. Fan, L. Liu, C. Yang, and L. Zhou, Opt. Express **24**, 1865 (2016).
5. J. M. Shainline, S. M. Buckley, N. Nader, C. M. Gentry, K. C. Cossel, J. W. Cleary, M. Popović, N. R. Newbury, S. W. Nam, and R. P. Mirin, Opt. Express **25**, 10322-10334 (2017).
6. C. Yin, Y. Chen, X. Jiang, Y. Zhang, Z. Shao, P. Xu, and S. Yu, Opt. Lett. .**41**, 4791-4794 (2016).
7. Z. Wu, Y. Chen, T. Zhang, Z. Shao, Y. Wen, P. Xu, Y. Zhang, and S. Yu, J. Opt. **19**(4), 045801 (2017).
8. P. Xu, Y. Chen, Z. Shao, Y. Zhang, T. Zhang, Z. Wu, C. Yang, L. Liu, L. Zhou, H. Chen, J. Liu, and S. Yu, in Asia Communications and Photonics Conference 2016, paper AF3F.4
9. C. G. Roeloffzen, L. Zhuang, C. Taddei, A. Leinse, R. G. Heideman, P. W. van Dijk, R. M. Oldenbeuving, D. A. Marpaung, M. Burla, and K. J. Boller, Opt. Express **21**, 22937 (2013).
10. Y. Liu, D. Marpaung, A. Choudhary, and B. J. Eggleton, in Conference on Lasers and Electro-Optics 2017, p. SM1O.7.
11. A. G. Griffith, R. K. Lau, J. Cardenas, Y. Okawachi, A. Mohanty, R. Fain, Y. H. Lee, M. Yu, C. T. Phare, C. B. Poitras, A. L. Gaeta, and Michal Lipson, Nat. Commun. **6**, 6299 (2014).
12. P. T. Lin, V. Singh, L. Kimerling, and A. M. Agarwal, Appl. Phys. Lett. **102**, 1345 (2013).
13. C. Herkommer, H. Guo, A. Billat, D. Grassani, M. Pfeiffer, M. Zervas, C.-S. Bres, and T. J. Kippenberg, in Conference on Lasers and Electro-Optics 2017, p. SM2K.6.
14. D. J. Moss, R. Morandotti, A. L. Gaeta, and M. Lipson, Nat. Photon. **7**, 597-607 (2013).
15. V. Brasch, E. Lucas, J. D. Jost, M. Geiselmann, and T. J. Kippenberg, Light-Sci. Appl. **6**, e16202 (2016).
16. A. Mohanty, M. Zhang, A. Dutt, S. Ramelow, P. Nussenzveig, and M. Lipson, Nat. Commun. **8**, 14010 (2016).
17. Q. Liu, X. Tu, K. W. Kim, J. S. Kee, S. Yong, K. Han, Y. J. Yoon, G. Q. Lo, and K. P. Mi, Sens. Actuator B Chem. **188**, 681-688 (2013).
18. R. Diekmann, Ø. I. Helle, C. I. Øie, P. Mccourt, T. R. Huser, M. Schüttpelz, and B. S. Ahluwalia, Nat. Photon. **11**, 322–328 (2017).
19. Y. Shen, S. Feng, X. Xie, J. Zang, S. Li, T. Su, K. Shang, W. Lai, G. Liu, S. J. Ben Yoo, and J. C. Campbell, Opt. Express **25**, 9521-9527 (2017).
20. C. Schuck, X. Guo, L. Fan, X. Ma, M. Poot, and H. X. Tang, Nat. Commun. **7**, 10352 (2016).
21. P. Dong, IEEE J. Sel. Topic Quantum Electron. **22**(6), 6100609 (2016).
22. H. Zhang, C. Li, X. Tu, X. Luo, M. Yu, and G. Q. Lo, Appl. Phys. A **115**, 79-82 (2014).
23. C. R. Doerr, L. Chen, Y. K. Chen, and L. L. Buhl, IEEE Photon. Technol. Lett. **22**, 1461-1463 (2010).
24. X. Zhao, D. Li, C. Zeng, G. Gao, Z. Huang, Q. Huang, Y. Wang, and J. Xia, J. Lightwave Technol. **34**, 1322-1327 (2016).
25. H. Zhang, C. Li, X. Tu, J. Song, H. Zhou, X. Luo, Y. Huang, M. Yu, and G. Q. Lo, Opt. Express **22**, 21800-21805 (2014).
26. W. D. Sacher, Y. Huang, L. Ding, B. J. Taylor, H. Jayatilleka, G. Q. Lo, and J. K. Poon, Opt. Express **22**, 10938 (2014).
27. J. Zou, Y. Yu, M. Ye, L. Liu, S. Deng, and X. Zhang, Opt. Express 23, 26305-26312 (2015).
28. Y. Chen, R. Halir, Í. Molina-Fernández, P. Cheben, and J. J. He, Opt. Lett. **41**, 5059-5062 (2016).
29. D. Taillaert, F. Van Laere, M. Ayre, W. Bogaerts, D. Van Thourhout, P. Bienstman, and R. Baets, J. J. Appl. Phys. **45**, 6071-6077 (2006).
30. E.-G. Neumann, "Single-Mode Fibers Fundamentals," Springer, 1988.
31. B. A. Dorin and W. N. Ye, Opt. Express **22**, 4547 (2014).

References

1. D. Thomson, A. Zilkie, J. E. Bowers, T. Komljenovic, G. T. Reed, L. Vivien, D. Marrismorini, E. Cassan, L. Virot, and J. M. Fédéli, "Roadmap on silicon photonics," J. Opt. **18**, 073003 (2016).
2. S. Romerogarcía, F. Merget, F. Zhong, H. Finkelstein, and J. Witzens, "Visible wavelength silicon nitride focusing grating coupler with AlCu/TiN reflector," Opt. Lett. **38**, 2521-2523 (2013).
3. A. Rahim, E. Ryckeboer, A. Subramanian, S. Clemmen, B. Kuyken, A. Dhakal, A. Raza, A. Hermans, M. Muneeb, and S. Dhoore, "Expanding the silicon photonics portfolio with silicon nitride photonic integrated circuits," J. Lightwave Technol. **35**(4), 639-649 (2017).
4. Z. Shao, Y. Chen, H. Chen, Y. Zhang, F. Zhang, J. Jian, Z. Fan, L. Liu, C. Yang, and L. Zhou, "Ultra-low temperature silicon nitride photonic integration platform," Opt. Express **24**, 1865 (2016).
5. J. M. Shainline, S. M. Buckley, N. Nader, C. M. Gentry, K. C. Cossel, J. W. Cleary, M. Popović, N. R. Newbury, S. W. Nam, and R. P. Mirin, "Room-temperature-deposited dielectrics and superconductors for integrated photonics," Opt. Express **25**, 10322-10334 (2017).
6. C. Yin, Y. Chen, X. Jiang, Y. Zhang, Z. Shao, P. Xu, and S. Yu, "Realizing topological edge states in a silicon nitride microring-based photonic integrated circuit", Opt. Lett. .**41**, 4791-4794 (2016).
7. Z. Wu, Y. Chen, T. Zhang, Z. Shao, Y. Wen, P. Xu, Y. Zhang, and S. Yu, "Design and optimization of optical modulators based on graphene-on-silicon nitride microring resonators", J. Opt. **19**(4), 045801 (2017).
8. P. Xu, Y. Chen, Z. Shao, Y. Zhang, T. Zhang, Z. Wu, C. Yang, L. Liu, L. Zhou, H. Chen, J. Liu, and S. Yu, "Hybrid integrated velocity matched travelling-wave InP/InGaAs photodetectors with silicon nitride waveguides", in Asia Communications and Photonics Conference 2016, OSA Technical Digest (Optical Society of America, 2016), paper AF3F.4
9. C. G. Roeloffzen, L. Zhuang, C. Taddei, A. Leinse, R. G. Heideman, P. W. van Dijk, R. M. Oldenbeuving, D. A. Marpaung, M. Burla, and K. J. Boller, "Silicon nitride microwave photonic circuits," Opt. Express **21**, 22937 (2013).
10. Y. Liu, D. Marpaung, A. Choudhary, and B. J. Eggleton, "Highly selective and reconfigurable Si_3N_4 RF photonic notch filter with negligible RF losses," in Conference on Lasers and Electro-Optics (Optical Society of America, San Jose, California, 2017), p. SM1O.7.
11. A. G. Griffith, R. K. Lau, J. Cardenas, Y. Okawachi, A. Mohanty, R. Fain, Y. H. Lee, M. Yu, C. T. Phare, C. B. Poitras, A. L. Gaeta, and Michal Lipson, "Silicon-chip mid-infrared frequency comb generation," Nat. Commun. **6**, 6299 (2014).
12. P. T. Lin, V. Singh, L. Kimerling, and A. M. Agarwal, "Planar silicon nitride mid-infrared devices," Appl. Phys. Lett. **102**, 1345 (2013).
13. C. Herkommer, H. Guo, A. Billat, D. Grassani, M. Pfeiffer, M. Zervas, C.-S. Bres, and T. J. Kippenberg, "A chip-based silicon nitride platform for mid-infrared nonlinear photonics," in Conference on Lasers and Electro-Optics (Optical Society of America, San Jose, California, 2017), p. SM2K.6.
14. D. J. Moss, R. Morandotti, A. L. Gaeta, and M. Lipson, "New CMOS-compatible platforms based on silicon nitride and Hydex for nonlinear optics," Nat. Photon. **7**, 597-607 (2013).
15. V. Brasch, E. Lucas, J. D. Jost, M. Geiselmann, and T. J. Kippenberg, "Self-referenced photonic chip soliton Kerr frequency comb," Light-Sci. Appl. **6**, e16202 (2016).
16. A. Mohanty, M. Zhang, A. Dutt, S. Ramelow, P. Nussenzveig, and M. Lipson, "Quantum interference between transverse spatial waveguide modes," Nat. Commun. **8**, 14010 (2016).
17. Q. Liu, X. Tu, K. W. Kim, J. S. Kee, S. Yong, K. Han, Y. J. Yoon, G. Q. Lo, and K. P. Mi, "Highly sensitive Mach–Zehnder interferometer biosensor based on silicon nitride slot waveguide," Sens. Actuator B Chem. **188**, 681-688 (2013).
18. R. Diekmann, Ø. I. Helle, C. I. Øie, P. Mccourt, T. R. Huser, M. Schüttpelz, and B. S. Ahluwalia, "Chip-based wide field-of-view nanoscopy," Nat. Photon. **11**, 322–328 (2017).
19. Y. Shen, S. Feng, X. Xie, J. Zang, S. Li, T. Su, K. Shang, W. Lai, G. Liu, S. J. Ben Yoo, and J. C. Campbell, "Hybrid integration of modified uni-traveling carrier photodiodes on a multi-layer silicon nitride platform using total reflection mirrors," Opt. Express **25**, 9521-9527 (2017).
20. C. Schuck, X. Guo, L. Fan, X. Ma, M. Poot, and H. X. Tang, "Quantum interference in heterogeneous superconducting-photonic circuits on a silicon chip," Nat. Commun. **7**, 10352 (2016).
21. P. Dong, "Silicon photonic integrated circuits for wavelength-division multiplexing applications," IEEE J. Sel. Topic Quantum Electron. 22(6), 6100609 (2016).
22. H. Zhang, C. Li, X. Tu, X. Luo, M. Yu, and G. Q. Lo, "High efficiency silicon nitride grating coupler," Appl. Phys. A **115**, 79-82 (2014).
23. C. R. Doerr, L. Chen, Y. K. Chen, and L. L. Buhl, "Wide Bandwidth Silicon Nitride Grating Coupler," IEEE Photon. Technol. Lett. **22**, 1461-1463 (2010).
24. X. Zhao, D. Li, C. Zeng, G. Gao, Z. Huang, Q. Huang, Y. Wang, and J. Xia, "Compact grating coupler for 700-nm silicon nitride strip waveguides," J. Lightwave Technol. **34**, 1322-1327 (2016).
25. H. Zhang, C. Li, X. Tu, J. Song, H. Zhou, X. Luo, Y. Huang, M. Yu, and G. Q. Lo, "Efficient silicon nitride grating coupler with distributed Bragg reflectors," Opt. Express **22**, 21800-21805 (2014).
26. W. D. Sacher, Y. Huang, L. Ding, B. J. Taylor, H. Jayatilleka, G. Q. Lo, and J. K. Poon, "Wide bandwidth and high coupling efficiency Si_3N_4-on-SOI dual-level grating coupler," Opt. Express **22**, 10938 (2014).
27. J. Zou, Y. Yu, M. Ye, L. Liu, S. Deng, and X. Zhang, "Ultra efficient silicon nitride grating coupler with bottom grating reflector," Opt. Express 23, 26305-26312 (2015).
28. Y. Chen, R. Halir, Í. Molina-Fernández, P. Cheben, and J. J. He, "High-efficiency apodized-imaging chip-fiber grating coupler for silicon nitride waveguides," Opt. Lett. **41**, 5059-5062 (2016).
29. D. Taillaert, F. Van Laere, M. Ayre, W. Bogaerts, D. Van Thourhout, P. Bienstman, and R. Baets, "Grating Couplers for Coupling between Optical Fibers and Nanophotonic Waveguides," J. J. Appl. Phys. **45**, 6071-6077 (2006).
30. E.-G. Neumann, "Single-Mode Fibers Fundamentals," Springer, 1988.
31. B. A. Dorin, and W. N. Ye, "Two-mode division multiplexing in a silicon-on-insulator ring resonator," Opt. Express **22**, 4547 (2014).